ELSEVIER

Nuclear Instruments and Methods in Physics Research B 140 (1998) 380–388

NIM B
Beam Interactions with Materials & Atoms

A TOF spectrometer for elastic recoil detection

J.K. Kim [a,*], Y.S. Kim [a], G.D. Kim [a], H.W. Choi [a], H.J. Woo [a], S.Y. Cho [a], C.N. Whang [b]

[a] *Korea Institute of Geology, Mining and Materials, 30 Kajung-dong, Yusung-gu, Taejon 305-350, South Korea*
[b] *Department of physics, Yonsei university, Seoul 120-749, South Korea*

Received 18 August 1997; received in revised form 3 November 1997

Abstract

A time-of-flight spectrometer was built for the ERD-TOF (Elastic Recoil Detection by Time Of Flight) and heavy ion RBS (Rutherford Backscattering Spectrometry) experiments with a 1.7 MV tandem Van de Graaff accelerator. The spectrometer consists of two time pick-off detectors and a SSB (Silicon Surface Barrier) detector with variable flight lengths. The time detector uses an electrode to accelerate and to focus the electrons from a thin carbon foil to a MCP (Micro Channel Plate). The advantage of this type of time detector is the good efficiency and no obstacles in the beam path at the cost of a small uncertainty in the flight length. The efficiency of the spectrometer was measured for the ions lighter than neon in the energy range of a few hundred keV to 7 MeV, and was better than 98% for the particles heavier than B. The intrinsic resolution of the time detector is about 220 ps. The time resolution of the spectrometer was measured as a function of incident particle type and energy. The mass resolution is below 1 amu for the particles of interest. © 1998 Elsevier Science B.V.

Keywords: TOF spectrometer; Time resolution; Detection efficiency; Mass resolution

1. Introduction

Since Chevarier [1] applied TOF spectrometer to heavy ion backscattering spectrometry in late 1970s, it has become a popular device for mass identification in ERD [2–11]. A TOF spectrometer usually consists of two time detectors and a energy detector. Commercially available SSBD can be used for the energy detector but time pick-off detectors are usually home-made. Since Stein [12] and Dietz [13] devised a time pick-off method using secondary electrons from thin films, the time detector has been developed into three categories according to the method of leading secondary electrons inside the time detector. First, electrons are accelerated by a biased grid [14–20]. In this type of detector flight lengths of secondary electrons are the same regardless of the electron's production point resulting in zero time spread. But because the grid can shield or disturb particles along the path, detection efficiency somewhat decreases and ghost signals can appear by the glanc-

* Corresponding author: Tel.: +82 42 868 3663; fax: +82 42 861 9727; e-mail: kimacc@rock25t.kigam.re.kr.

PII S0168-583X(98)00007-X

ing scattering. Second, using the MCP with the central hole without any grid, possible problems occurred from the grid can be eliminated [21–24]. But the time resolution and efficiency are inevitably degraded. Third, by use of the uniform magnetic field and quart-turn collimator, isochronous transport of secondary electrons is possible [25,26]. Good time resolution can be achieved at the cost of efficiency.

In this work, for the pursuit of both excellent time resolution and high detection efficiency, we designed a "tilted gridless" time detector shown in Fig. 1. The spectrometer is used for the TOF measurement in the elastic recoil detection of light elements.

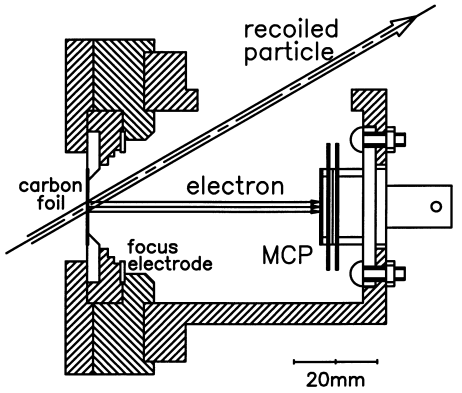

Fig. 1. Schematic view of the KIGAM time detector.

2. TOF spectrometer

The TOF spectrometer consists of two identical time detectors and one energy detector as shown in Fig. 2. The energy detector is a low ohmic (400 Ω cm) SSB detector. As usual in heavy ion detection, the SSB detector was over-biased for the quick time response and for the alleviation of pulse height defect (PHD) [27–29]. Each time detector is located in a 200 mm × 200 mm rectangular shape chamber and the SSB detector is positioned at the rear side of the stop chamber. The flight length can be varied by replacing the connecting pipe between the two time detector chambers. A tungsten collimator of 5 mm diameter in front of SSBD defines the solid angle of spectrometer. An isolation valve is inserted between the target chamber and the spectrometer to shorten the evacuation time after target change. The solid angle of spectrometer is about 1.6×10^{-5} steradian with the typical arrangement of 0.745 m flight length. Base pressure of the target chamber was less than 4×10^{-7} torr when using the liquid nitrogen trap. The bias voltage of the electrodes in the time detector was determined via the backscattering experiment using 3.6 MeV carbon as shown in Fig. 3. Optimum voltages of front and back side of MCP were decided to be −2.3 and −0.1 kV, respectively. Carbon foils with a typical thickness of 5 μg/cm^2 (Goodfellow, England) and 10 μg/cm^2 (Nilaco, Japan) were used.

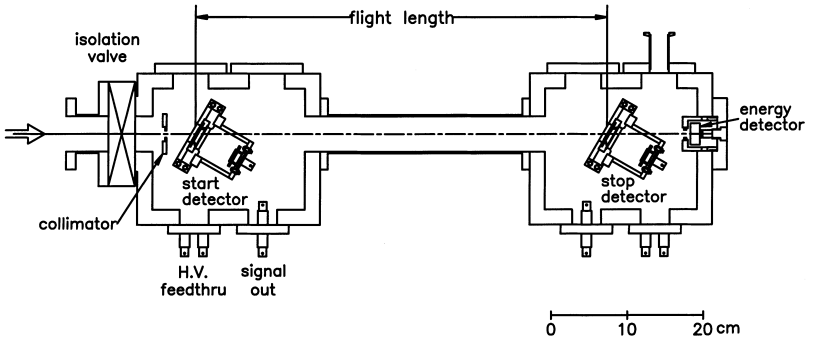

Fig. 2. TOF spectrometer with two time pick-off detectors and a SSB energy detector.

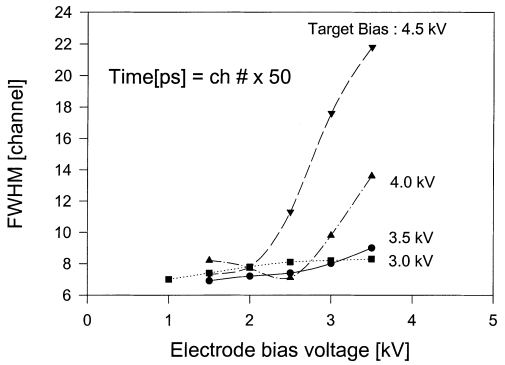

Fig. 3. Optimization of the bias voltages at the carbon foil and focusing electrode. Time resolutions are measured by backscattered carbon ion from 5 nm Au on silicon.

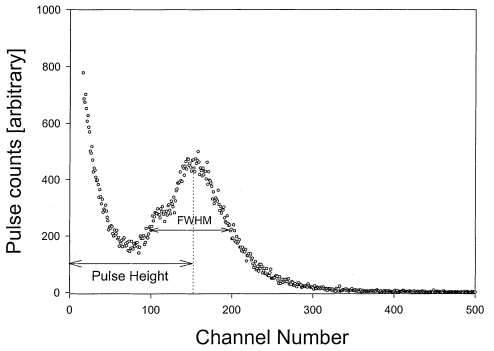

Fig. 4. Pulse height distribution of the time detector for 4 MeV oxygen.

3. Experimental

Detection efficiency(η_S) of the spectrometer is measured by the ratio of triple coincidence to the SSBD signal as follows:

$$\eta_S \equiv \frac{T_1 * T_2 * T_3}{T_3}. \quad (1)$$

T_1 and T_2 are signals from the start and stop detector and T_3 is that of the SSBD. Because the pulse height resolution (PHR) of the MCP (Hamamatshu, F4655-10) is about 45% as shown in Fig. 4, perfect separation of true signals from noise is impossible. Fig. 5 is the efficiency curve of fluorine particles versus threshold voltage. As the threshold level goes up, the discriminator starts to lose true signals seriously. We define the point at which the spectrometer efficiency goes down 98% of maximum value as the critical voltage and all the measurements were performed below this value. Table 1 is the measured critical threshold voltage from proton to fluorine. Since fabricated TOF spectrometer will be applied for 10 MeV ^{35}Cl induced ERD system, efficiencies were measured within the energy region of recoiled light el-

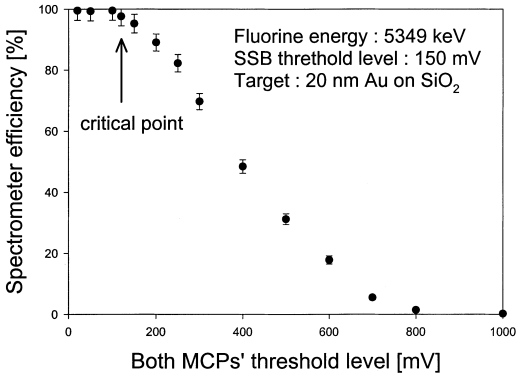

Fig. 5. Efficiencies of the spectrometer as a function of CFD threshold level. Both discriminators were set for the same values.

Table 1
Critical threshold voltage and the efficiencies of the spectrometer

Projectile	Energy (MeV)	Threshold voltage (mV)	Efficiency (η_s, %)
^{1}H	1.029	25 [a]	22
^{6}Li	3.932	25 [a]	94
^{10}B	5.004	50	98
^{12}C	5.179	80	98
^{19}F	5.349	180	98

[a] minimum threshold voltage provided by the used constant fraction discriminator.

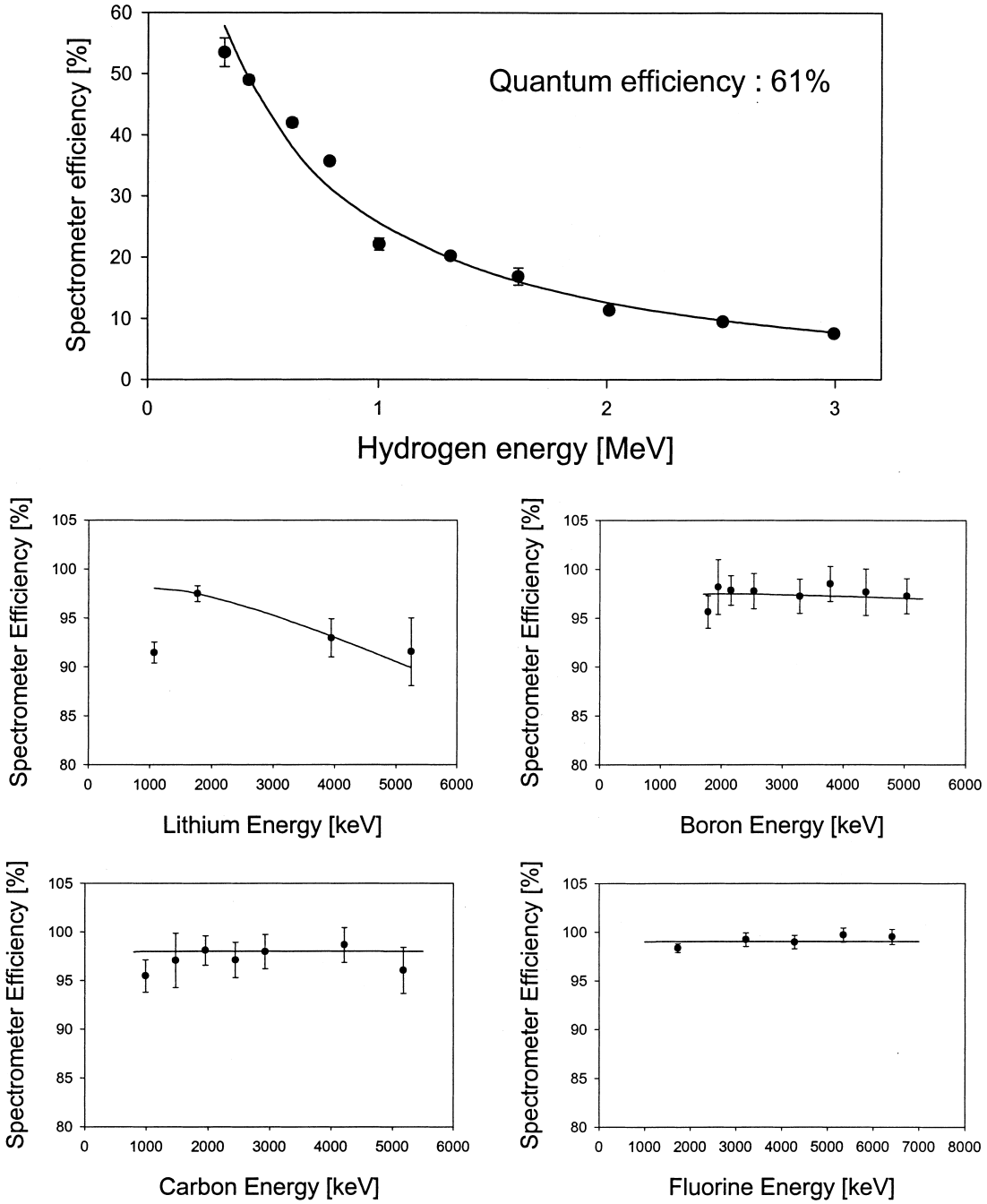

Fig. 6. Detection efficiencies of the TOF spectrometer for light elements within the energy region of the 10 MeV ^{35}Cl induced recoils.

ements. Fig. 6 shows the efficiencies of light element projectiles as a function of their kinetic energies.

Time resolution has been measured using the backscattered time spectrum from a Au target [30–33]. Backscattering spectra were measured at

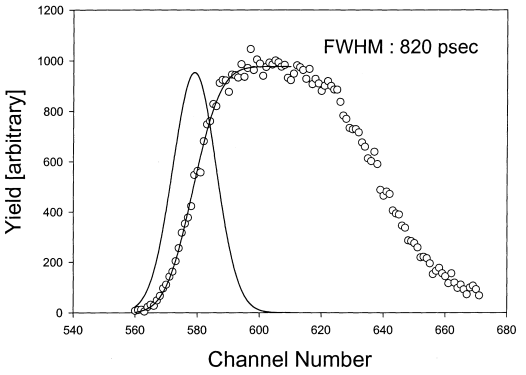

Fig. 7. Time spectrum of 4.2 MeV fluorine backscattered from a thick Au target.

140° scattering angle with the 60° tilted 40 nm Au target on Si. Fig. 7 is the time spectrum of 4.2 MeV fluorine incidence. Time resolution is obtained by fitting the leading edge of the Au spectrum with the Gaussian cumulative distribution function. Simultaneous determination of intrinsic time resolution and contributions from the energy spread is possible by the measurements at different incident energies. Fig. 8 shows the measured time resolution of three projectiles at 0.745 m flight length.

4. Result and discussion

Detection efficiency, Weller model [34]. The performance of the time detector is similar to that of a SSBD in the aspect that it has a wide dynamic range – energy and species – and its response is independent of charge state. But the efficiency of time detector depends on the projectile and its energy. In other words the detection efficiency of time pick-off detector depends strongly on the number of secondary electrons produced in the carbon foil. The intrinsic efficiency of time detector is defined as the probability to get a true signal when the projectile passes through the carbon foil. The number of secondary electrons produced by energetic particles in the carbon foil [35,36] is given by Rothard [37] as follows:

$$\gamma_C = \Lambda S_C. \tag{2}$$

Here S_C is the electronic stopping power and Λ is the proportional coefficient. Rothard's experimental values are 0.022 nm/eV for proton, 0.015 nm/eV for helium and 0.011 nm/eV for heavier particles. The number of secondary electrons is saturated for carbon foils thicker than 5 μg/cm^2 [38], so the detection efficiency of a TOF spectrometer using two time detectors can be given as [39]

$$\eta = (1 - e^{-\lambda_1 \Lambda_1 S_1}) f (1 - e^{-\lambda_2 \Lambda_2 S_2}), \tag{3}$$

where f is the transport efficiency between the two time detectors [34] and λ is the quantum efficiency of the MCP [40]. Because two detectors are identical and transport efficiency is 100%, the efficiency of spectrometer is expressed by

$$\eta_S = \eta / f = (1 - e^{-\lambda \Lambda S})^2. \tag{4}$$

Fitting the experimental values by Weller's efficiency model with Ziegler's stopping data [41], the resulting quantum efficiency was 61%. In the case of proton, average secondary electron yield in the carbon foil is 0.44 for 3 MeV and 2 for 0.3 MeV. So it is easy to expect large change of efficiency along its kinetic energy. But it is fortunate for the quantitative analysis of light elements that the efficiency behavior can be predicted by Weller's model as shown in Fig. 6. For particles heavier than Li, detection efficiencies are better than 94% within the interested energy region.

Intrinsic time resolution. The time resolution of the spectrometer comprises two contributions [11,33]. One is the intrinsic time resolution which is independent of experimental environment (spe-

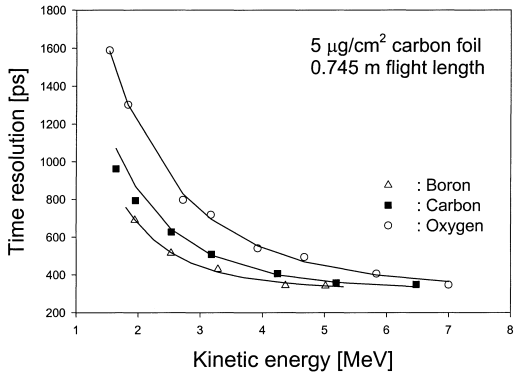

Fig. 8. Time resolutions of ^{10}B, ^{12}C and ^{16}O using 5 μg/cm^2 carbon foil. Flight length was fixed at 0.745 m.

cies of projectile, energy, flight length of the spectrometer etc.). The intrinsic time resolution includes the flight time spread of secondary electron, different time delay in MCP channel and the noise in the electronics. The other originates from the energy spread [42] caused before the spectrometer. These two terms contribute to total time resolution (Δt) quadratically as

$$(\Delta t)^2 = (36.1\ l\ \Delta E)^2 \frac{M}{E^3} + (\Delta t_i)^2, \tag{5}$$

where l is the flight length (m), E the projectile energy (MeV), M the mass (amu) and Δt_i the intrinsic time resolution (ns). The energy spread caused before the spectrometer includes following factors.

1. *Beam energy spread,* ΔE_{Beam}: It is due to the terminal voltage fluctuation of the accelerator. When the stability of high voltage terminal is δTV and charge state is q, then ΔE_{Beam} becomes $(1+q) * (\delta TV)$. δTV of KIGAM tandem VDG is less than ± 1 kV.

2. *Geometrical contribution,* ΔE_{Geom}: The finite size of the beam on the target and detector cause the spread in the scattering angle. The energy spread of the detected particles caused by this scattering angle difference is defined as ΔE_{Geom} and given as follows when circular shape beam and detector is assumed [43]:

$$\Delta E_{\mathrm{Geom}} = E_0 \cdot \frac{\partial K}{\partial \theta} \cdot \delta\theta,$$

$$(\delta\theta)^2 = \left(\frac{g_d W}{L_D}\right)^2 + \left(\frac{g_b d \sin\beta}{L_D \sin\alpha}\right)^2, \tag{6}$$

where E_0 is the incident energy and K, the scattering kinematic factor. θ is the scattering angle and α, β are inlet and outlet angle to the sample normal. L_D denotes the distance between the sample and stop detector and W, d are the effective diameter of the beam on the target and of the stop detector. g_d and g_b are 0.59 when circular shape is assumed [43].

3. *Energy straggling in the start carbon foil,* ΔE_{Stra}: To calculate the straggling effect in the carbon foil Yang's empirical formula [44] was used.

$$(\Delta E_{\mathrm{Stra}}/\Omega_{\mathrm{Bohr}})^2 = \left(Z_1^{4/3}/Z_2^{1/3}\right) C_1 \Gamma / \{(\varepsilon - C_2) + \Gamma^2\}, \tag{7}$$

$$\Gamma = C_3(1 - e^{-C_4\varepsilon}),$$

$$\varepsilon = E/Z_1^{3/2} Z_2^{1/2},$$

where Ω_{Bohr} is the Bohr straggling and E is the projectile energy per nucleon in MeV. C_i $(i = 1\text{–}4)$ are fitted constants for solid by Yang et al. Subscript 1 means the projectile and 2 indicates carbon foil.

4. *Non-uniform energy loss in the carbon foil,* ΔE_{Foil}: The energy spread due to the non-uniform carbon foil can be expressed as

$$\Delta E_{\mathrm{Foil}} = h\left(\frac{dE}{dx}\right) x_{\mathrm{Carbon}}, \tag{8}$$

where x_{Carbon} is the path length of projectile in the carbon foil and h is a fitting parameter which is a measure of non-uniformity.

These four terms are independent of each other. So the energy spread occurred before the spectrometer is given by

Table 2
Fitting results for the intrinsic time resolution (Δt_i) and foil non-uniformity factor (h)

Flight particle	Intrinsic time resolution (Δt_i, ps)	Foil non-uniformity level (h, %)	Flight length (m)
^{10}B	324	33	0.745
^{12}C	291	32	0.445
^{19}F	309	24	0.445
Average	308.0 ± 13.5	29.7 ± 4.0	For 10 μg/cm^2
^{10}B	313	54	0.745
^{12}C	312	52	0.745
^{16}O	312	54	0.745
Average	312.3 ± 0.5	53.3 ± 0.9	For 5 μg/cm^2

$$(\Delta E_S)^2 = (\Delta E_{Beam})^2 + (\Delta E_{Geom})^2 + (\Delta E_{Stra})^2 + (\Delta E_{Foil})^2. \quad (9)$$

The measured values are fitted by the least square scheme with two parameters – intrinsic time resolution (Δt_i) and thickness non-uniform level (h). The fitting results are shown in Table 2.

The contributions from the energy spread are amplified with the flight length and projectile velocity. But as shown in Eq. (5) this effect diminishes as the projectile's kinetic energy increases and time resolution approaches to the intrinsic value, 310 ps. The contributions to the spectrometer time resolution in case of oxygen are shown in Fig. 9. Foil non-uniformity effect has a large influence below 2 MeV and above this energy intrinsic time resolution is absolutely dominant. The non-uniformity level of carbon foils by fitting show 53% and 30% for 5 μg/cm^2 and 10 μg/cm^2, respectively. These values correspond to about 15 and 13.2 nm surface roughness. The non-uniformity level (h) resulting from the parameter fitting of time resolution agrees well with the AFM (Atomic Force Microscope) image of surface roughness in Fig. 10.

Energy and mass resolution. Energy of a projectile can be obtained either from the flight time after mass identification or from direct reading of the SSBD. When the particle energy to be detected is small, it is often advantageous to obtain energy information from flight time. In this case energy resolution is given by the quadratic summation of the intrinsic time resolution and the energy spread in Eq. (9) i.e.,

$$(\Delta E_{TOF})^2 = \left(\frac{\Delta t_i}{36.1 * l}\right)^2 \frac{E^3}{M} + (\Delta E_S). \quad (10)$$

The energy resolutions calculated in this way are shown in Fig. 11. When the energy resolution of light element for SSBD is about 100 keV (for example oxygen), the flight time-deduced energy resolution is better than that of SSBD below 5 MeV.

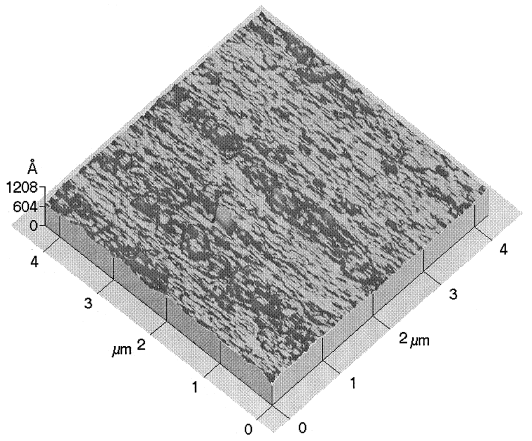

Fig. 10. Surface AFM image of carbon film used in the time detector.

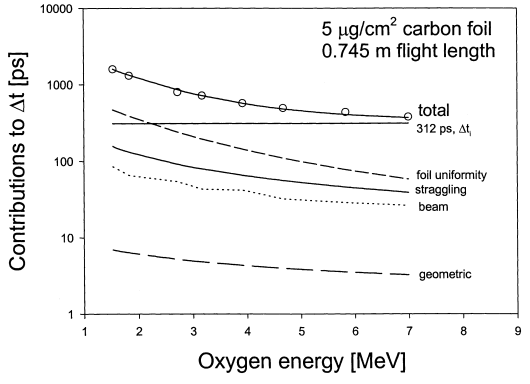

Fig. 9. Contributions of the intrinsic time resolution, energy straggling, thickness non-uniformity of the carbon foil, geometric angle spread and incident beam energy spread to the total time resolution calculated for ^{16}O with various incident energies. Points are measured values.

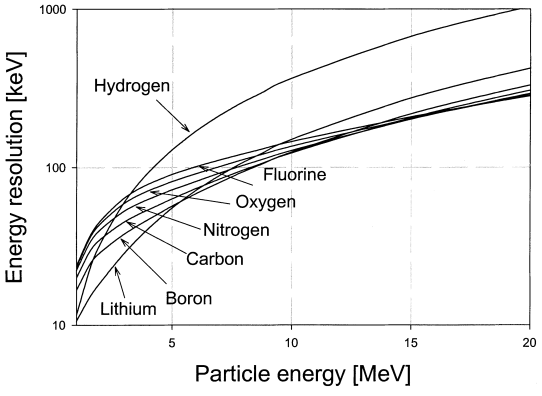

Fig. 11. Energy resolutions converted from the corresponding time resolutions of the TOF spectrometer.

Therefore if this TOF spectrometer is applied to 33° ERD experiment with the 10 MeV ^{35}Cl, it is advantageous to fetch the energy information from the flight time. The mass resolution (ΔM) of TOF spectrometer is given by

$$\left(\frac{\Delta M}{M}\right)^2 = \left(\frac{\Delta E}{E}\right)^2 + \left(\frac{2\Delta t}{t}\right)^2 + \left(\frac{2\Delta l}{l}\right)^2, \quad (11)$$

here, ΔE is the energy resolution of SSBD, Δt is time resolution and Δl is the uncertainty of flight length. Assuming that the energy resolution (ΔE) follows $E^{1/3}$ rule [45] and relative flight length uncertainty ($\Delta l/l$) is 0.1%, then the mass resolution of TOF spectrometer can be estimated as in Fig. 12. It is good enough for the separation of elements lighter than fluorine.

5. Conclusion

A TOF spectrometer consisting of a SSBD and two identical time pick-off detectors has been fabricated, and its characteristics of time resolution and detection efficiency were investigated for the recoiled light particles induced by 10 MeV ^{35}Cl via scattering experiments. Detection efficiencies are better than 98% for projectiles heavier than boron. For Li and proton, efficiencies agree well with Weller's model. The intrinsic time resolution of the spectrometer is 310 ps, which means the intrinsic resolution of each time detector is about 220 ps. The time resolution of KIGAM time-pick-off detector is suited for the application to the analysis of light element recoils induced by ^{35}Cl in thin films. KIGAM TOF spectrometer has a good mass resolution for elements lighter than Mg. Compared with the SSBD signal, flight time deduced energy information is better to use in the recoil experiment. Although the time resolution is enough to separate light element recoils induce by 10 MeV ^{35}Cl, better time resolution is desired if the spectrometer is to be applied to the heavy ion RBS.

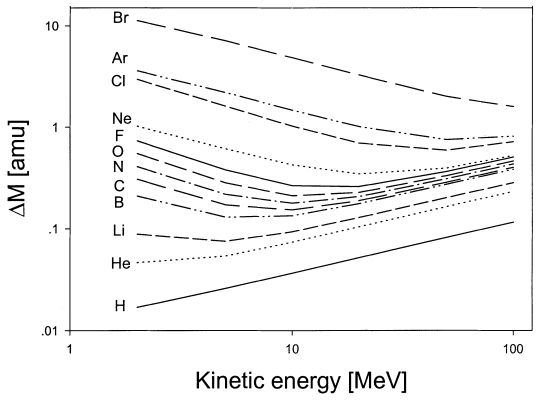

Fig. 12. Mass resolution of the TOF spectrometer calculated by assuming 0.745 m flight length and using $E^{1/3}$ rule as the SSBD energy resolution [45].

References

[1] J.P. Thomas, M. Fallavier, D. Ramdane, N. Chevarier, A. Chevarier, Nucl. Instr. and Meth. 218 (1983) 125.
[2] J.F. Curri, P. Depelsenaire, P. Paquin, M.R. Wertheimer, A. Yelon, Can. J. Phys. 61 (1983) 582.
[3] R. Groleau, S.C. Gujrathi, J.P. Martin, Nucl. Instr. and Meth. 218 (1983) 11.
[4] R. Groloau, J.F. Curri, M.R. Wertheimer, J.E. Klemberg-Sapieha, K.M. Wang, Thin Solid Films 136 (1986) 85.
[5] S.C. Gujrathi, P. Aubry, L. Lemay, J.P. Martin, Can. J. Phys. 65 (1987) 950.
[6] S.C. Gujrathi, S. Bultena, Nucl. Instr. and Meth. B 64 (1992) 789.
[7] S.C. Gujrathi, D. Poitras, J.E. Klemberg-Sapieha, L. Martinu, Nucl. Instr. and Meth. B 118 (1996) 560.
[8] C. Janicki, P.F. Hinrichsen, S.C. Gujrathi, J. Brebner, J.P. Martin, Nucl. Instr. and Meth. B 34 (1988) 484.
[9] K. Oxorn, S.C. Gujrathi, S. Bultena, L. Cliché, J. Miskin, Nucl. Instr. and Meth. B 45 (1990) 166.
[10] H.J. Whitlow, G. Possnert, C.S. Petersson, Nucl. Instr. and Meth. B 27 (1987) 448.
[11] H.J. Whitlow, G. Possnert, C.S. Petersson, K.J. Reeson, P.L.F. Hemment, Appl. Phys. Lett. 52 (1988) 1871.
[12] W.E. Stein, R.B. Leachman, Rev. Sci. Instr. 27 (1956) 1049.
[13] E. Dietz, R. Bass, A. Reiter, V. Friedland, B. Hubert, Nucl. Instr. and Meth. 97 (1971) 581.
[14] H. Pleyer, B. Kohlmeyer, W.F.W. Schneider, R. Bock, Nucl. Instr. and Meth. 96 (1971) 263.
[15] T.M. Comier, R.S. Galik, E.R. Cosman, A.J. Lazzarini, Nucl. Instr. and Meth. 119 (1974) 145.
[16] S. Lunardi, M. Morando, C. Signorini, F.G. Prete, W. Starzecki, A.M. Stefanini, Nucl. Instr. and Meth. 196 (1982) 223.
[17] G. D'Erasmo, V. Patcchio, A. Pantaleo, Nucl. Instr. and Meth. A 234 (1985) 91.
[18] W. Starzecki, A.M. Stefanini, S. Lunardi, C. Signorini, Nucl. Instr. and Meth. 193 (1982) 499.

[19] G. Gabor, W. Schimmerling, D. Greiner, F. Bisher, P. Lindstrom, Nucl. Instr. and Meth. 130 (1975) 65.
[20] I. Girard, M. Bolori, Nucl. Instr. and Meth. 140 (1977) 279.
[21] E. Weissenberg, W. Kast, F. Goennenwein, Nucl. Instr. and Meth. 163 (1979) 359.
[22] T. Nakagawa, W. Bohne, Nucl. Instr. and Meth. A 271 (1988) 523.
[23] A. Oed, G. Barreau, F. Goennenwein, P. Perrin, C. Ristori, Nucl. Instr. and Meth. 179 (1981) 265.
[24] T. Nakagawa, K.Y. Nakagawa, Jpn. J. Appl. Phys. 28 (1989) 498.
[25] A.M. Zebelman, W.G. Meyer, K. Halbach, A.M. Poskanzer, R.G. Sextro, G. Gabor, D.A. Landis, Nucl. Instr. and Meth. 141 (1977) 439.
[26] J.D. Bowman, R.H. Heffner, Nucl. Instr. and Meth. 148 (1978) 503.
[27] L. Cliché, S.C. Gujrathi, L.A. Hamel, Nucl. Instr. and Meth. B 45 (1990) 270.
[28] H. Funaki, M. Mashimo, M. Shimizu, Y. Oguri, E. Arai, Nucl. Instr. and Meth. B 56/57 (1991) 975.
[29] D. Come, J. Davies, Nucl. Instr. and Meth. B 67 (1992) 93.
[30] A. Chevarier, N. Chevarier, S. Chiodelli, Nucl. Instr. and Meth. 189 (1981) 525.
[31] A. Chevarier, N. Chevarier, Nucl. Instr. and Meth. 218 (1983) 1.
[32] A. Chevarier, N. Chevarier, M. Stern, D. Lamouche, P. Clechet, J.R. Martin, P. Person, Nucl. Instr. and Meth. B 13 (1986) 207.
[33] M. Doebeli, P.C. Haubert, R.P. Livi, S.J. Spicklemire, D.L. Weather, T.A. Tombrello, Nucl. Instr. and Meth. B 47 (1990) 148.
[34] J.H. Arps, R.A. Weller, Nucl. Instr. and Meth. B 90 (1994) 547.
[35] E.J. Sternglass, Phys. Rev. 108 (1985) 263.
[36] C.R. Shi, H.S. Toh, D. Lo, R.P. Livi, M.H. Mendenhall, D.Z. Zhang, Nucl. Instr. and Meth. B 9 (1985) 263.
[37] H. Rothard, K. Kroneberger, A. Clouvas, E. Veje, P. Lorenzen, N. Keller, J. Kemmler, W. Meckbach, K.O. Groenveld, Phys. Rev. A 41 (1990) 2521.
[38] K. Kroneberger, A. Clouvas, G. Schluessel, P. Koscher, J. Kemmler, H. Rothard, C. Biedermann, O. Hei, M. Burkhard, O. Groeneveld, Nucl. Instr. and Meth. B 29 (1988) 621.
[39] R.A. Weller, J.H.A. Pedersen, M.H. Mendenhall, Nucl. Instr. and Meth. B 29 (1988) 621.
[40] G.W. Fraser, Nucl. Instr. and Meth. 206 (1983) 445.
[41] J.F. Ziegler, J.P. Biersack, U. Littmark, The Stopping and Range of Ions in Solids, vol. 1, Pergamon Press, New York, 1985.
[42] T.M. Stanescu, J.D. Meyer, H. Baumann, K. Bethe, Nucl. Instr. and Meth. B 50 (1990) 167.
[43] D. Dieumegard, D. Dubreuil, G. Amsel, Nucl. Instr. and Meth. 166 (1979) 431.
[44] Q. Yang, D.J. O'Connor, Z. Wang, Nucl. Instr. and Meth. B 61 (1991) 149.
[45] P.F. Hinrichsen, D.W. Hetherington, S.C. Gujrathi, L. Cliché, Nucl. Instr. and Meth. B 45 (1990) 275.